Mechanistic origin of cell-size control and homeostasis in bacteria

Fangwei Si[1†], Guillaume Le Treut[1†], John T. Sauls[1], Stephen Vadia[2], Petra Anne Levin[2], Suckjoon Jun[1,2,*]

[1] Department of Physics, University of California San Diego, La Jolla, California, 92093, USA

[2] Department of Biology, Washington University in St. Louis, Saint Louis, Missouri, 63130, USA

[3] Section of Molecular Biology, Division of Biology, University of California San Diego, La Jolla, California, 92093, USA

* To whom correspondence should be addressed; E-mail: suckjoon.jun@gmail.com.

† Contributed equally.

Evolutionarily divergent bacteria share a common phenomenological strategy for cell-size homeostasis under steady-state conditions. In the presence of inherent physiological stochasticity, cells following this "adder" principle gradually return to their steady-state size by adding a constant volume between birth and division regardless of their size at birth. However, the mechanism of the adder has been unknown despite intense efforts. In this work, we show that the adder is a direct consequence of two general processes in biology: (1) threshold -- accumulation of initiators and precursors required for cell division to a respective fixed number, and (2) balanced biosynthesis -- maintenance of their production proportional to volume growth. This mechanism is naturally robust to static growth inhibition, but also allows us to "reprogram" cell-size homeostasis in a quantitatively predictive manner in both Gram-negative *Escherichia coli* and Gram-positive *Bacillus subtilis*. By generating dynamic oscillations in the concentration of the division protein FtsZ, we were able to oscillate cell size at division and systematically break the adder. In contrast, periodic induction of replication initiator protein DnaA caused oscillations in cell size at initiation, but did not alter division size or the adder. Finally, we were able to restore the adder phenotype in slow growing *E. coli*, the only known steady-state growth condition wherein *E. coli* significantly deviates from the adder, by repressing active degradation of division proteins. Together these results show that division and replication are independently controlled, and that division processes exclusively drive cell-size homeostasis in bacteria.

INTRODUCTION

Cellular physiology is composed of inherently stochastic processes (Kiviet *et al*. 2014). Cell size at birth can fluctuate due to asymmetric division events or alterations in the timing or speed of constriction. Without homeostatic control, cell size in a continuous lineage would diverge with each division cycle. Evolutionarily divergent organisms ensure size homeostasis at the single-cell level by following a phenomenological principle known as the "adder" (Campos *et al*. 2014; Taheri-Araghi *et al*. 2014; Di Talia *et al*. 2007; Santi *et al*. 2013; Iyer-Biswas *et al*. 2014; Deforet *et al*. 2015; Logsdon *et al*. 2017; Soifer *et al*. 2016; Chandler-Brown *et al*. 2017; Varsano *et al*. 2017; Cadart *et al*. 2018; Jun *et al*. 2015; Sauls *et al*. 2016). A central property of the adder is that newborn cells deviating from the average size at birth add a nearly fixed volume between birth and division, allowing them to exponentially converge to the population average in each division cycle (Fig. 1). The adder sharply contrasts with a "sizer," in which cells divide when they reach a fixed size. The adder principle has been extended to eukaryotes from yeast (Soifer *et al*. 2016; Chandler-Brown *et al*. 2017; Jun *et al*. 2015) to mammalian cells (Varsano *et al*. 2017; Cadart *et al*. 2018) that have long been considered as sizers employing cell-cycle checkpoints.

The identification of the "adder" represented a major shift in our understanding of cell-size homeostasis (Jun *et al*. 2018; Willis and Huang 2017). Naturally, many models have been proposed to explain the mechanistic origin of the adder phenotype. Most of these models can be classified into different groups by each model's proposed implementation point of size control on the cell cycle. For example, recent works have suggested that the adder is governed by a replication-initiation-centric mechanism and division timing is determined by initiation in individual cells (Amir 2017). These models are based on the observation that cell size at initiation of DNA replication is invariant (Donachie 1968) at both single-cell (Wallden *et al*. 2016) and population level (Si *et al*. 2017). These models are in contrast to a division-centric view of size homeostasis proposed earlier based on computer simulations (Campos *et al*. 2014) or biological constraints imposed on cellular resource allocation to division proteins (Taheri-Araghi *et al*. 2014; Basan *et al*. 2015; Bertaux *et al*. 2016). Theoretical combination of replication and division controls has also been suggested at the phenomenological level (Osella *et al*. 2014; Micali *et al*. 2018a). Alternatively, cell shape, or more specifically the surface-to-volume ratio of the cell, has also been suggested as the determining factor for size control (Harris and Theriot 2016).

In this work, we explain the mechanistic origin of cell-size homeostasis common to *E. coli* and *B. subtilis*, bacteria that diverged over a billion years ago. Specifically, we show that the adder phenotype is a direct consequence of two general processes in biology (i) [threshold] accumulation of division initiators and precursors to a fixed threshold number per cell; and (ii) [balanced biosynthesis] their production is proportional to the growth of cell volume under steady-state condition. This mechanism allows us not only to "break" but also to "restore" the adder phenotype in a predictive manner under all major growth conditions.

Before proceeding to our results, we want to clarify the terminology. We use the term "cell-size control" for how cells determine their absolute size, and "cell-size homeostasis" for how cells correct deviations in size under steady-state growth. The two concepts are therefore closely related, yet differ with regard to whether emphasis is given to the requirement for threshold (for size control) or for balanced biosynthesis (for size homeostasis).

RESULTS AND DISCUSSION

Tracking replication and division cycles at the single-cell level

To illuminate the mechanisms underlying the adder principle, we performed a series of single-cell growth and cell-cycle tracking experiments under various growth conditions. We used a functional fluorescently-labeled replisome protein (DnaN-YPet) to image replication cycles, and a microfluidic mother machine to follow continuous lineages during steady-state growth (Wang *et al*. 2010; Taheri-Araghi *et al*. 2014) (Fig. 1A, Fig. S1; Methods; Supplemental Information II.A).

A major technical challenge arises in studying replication dynamics when two replisome foci spatially overlap, which makes it difficult to analyze overlapping replication cycles. To resolve this issue, we tracked multiple replication forks from initiation to termination by extending previous imaging methods (Wallden *et al*. 2016; Adiciptaningrum *et al*. 2015; Mangiameli *et al*. 2017; Logsdon *et al*. 2017) using the "intensity weighting" techniques (Holden *et al*. 2011; Cox *et al*. 2011) developed for super-resolution microscopy. This method allowed us to resolve overlapping replisome foci based on the number of peaks measured in the intensity distribution (Fig. 1B; see Supplemental Information II.D).

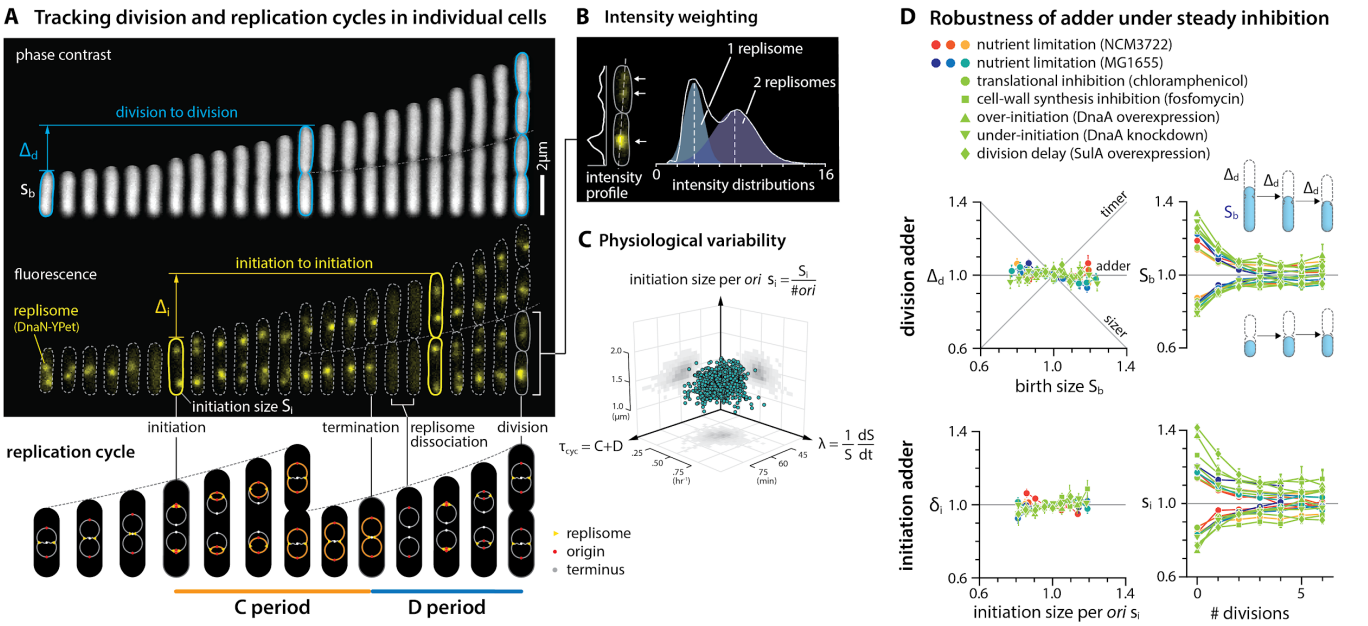

Figure 1: *E. coli* is both the initiation adder and division adder, and both are robust to static inhibition of growth and biosynthesis.

(A) Division adder vs. initiation adder. Upper: Δ_d is the added size between birth size S_b and division size S_d , and Δ_i is the added size between total cell size at two consecutive initiations. Initiation size per *ori* s_i is defined as the initiation size S_i per number of replication origins, and δ_i represents Δ_i per origin. Cell length is used as cell size because cell width is mostly constant (Taheri-Araghi *et al*. 2014) (Figs. S3 and S4). Lower: Illustration of the replication cycle with two overlapping cell cycles. The growth condition is MOPS minimal medium with 0.2 % glucose.

(B) Resolving overlapping foci using intensity weighting. The two peaks of intensity distribution of fluorescence foci indicate 1 and 2 replisomes, respectively (Supplemental Information II.D).

(C) Three major measured physiological parameters, growth rate λ, τ_{cyc}, and s_i all show variability and cross-correlation between 8%-20%. Each dot represents the data measured from one division cycle of a single cell.

(D) Under static biosynthetic inhibition, *E. coli* robustly corrects deviations in initiation size per *ori* and division size following initiation adder and division adder, respectively. Each dot is the binned data and error bar indicates standard error of mean, same for other figures. In the correlation plots, the variables are normalized by their means. See sample size in Supplemental Information II.C.

E. coli is an 'initiation adder' and a 'division adder', both robust to static inhibition of biosynthesis

Observation of wild type cells growing at steady state indicated the presence of two types of adder in *E. coli*: one functioning at division (hereafter a "division adder") and the other at replication initiation (an "initiation adder") (Fig. 1). Parallel to the "division adder" (Campos *et al*. 2014; Taheri-Araghi *et al*. 2014), the "initiation adder" is characterized by the addition of a nearly constant size per origin between consecutive replication cycles. This ensures that deviations in initiation size per *ori* exponentially converge to the population average in each replication cycle (Sompayrac and Maaløe 1973; Logsdon *et al*. 2017) (Fig. 1D).

We next wanted to clarify the contribution of initiation and division to their respective adders. We utilized either tunable CRISPR interference (Li *et al*. 2016; Si *et al*. 2017] to inhibit expression of *dnaA*, encoding the major bacterial DNA replication initiation protein, or an inducible-repressive promoter to modulate expression of a division inhibitor protein SulA. As expected, delays in replication and division both increased the average cell size (Fig. S2B). However, neither perturbation had a detectable effect on the initiation adder or division adder (Fig. 1D).

We also tested whether perturbations to global biosynthesis affect cell-size homeostasis, as they cause *E. coli* to deviate from the "growth law," namely the well-established exponential relationship between the average cell size and the nutrient-imposed growth rate (Schaechter *et al*. 1958; Si *et al*. 2017). In addition, previous work proposed accumulation of a fixed amount of cell-wall precursors as the mechanism of division adder (Harris and Theriot 2016). We thus used either chloramphenicol to target ribosomes or fosfomycin to target synthesis of cell-wall precursors, with the expectation that cells treated with these antibiotics would no longer exhibit adder. In both cases, however, we found that defects in these major biosynthetic pathways did not affect either type of adder (Fig. 1D). Together these data show that *E. coli* possess the capacity to buffer steady inhibitions of cell cycle processes or general biosynthesis to maintain robust size homeostasis.

Exploration of the physiological space using stochastic simulations identify experimental conditions whereby *E. coli* should deviate from the adder

The robustness of adder posed unforeseen challenges for our attempts to identify the biological processes underlying adder. Although we considered other types of perturbations or genetic screens, we realized that the physiological space was unrealistically large for brute-force search via single-cell time-lapse experiments. To circumvent the experimental challenges, we resorted to single-cell stochastic simulations and surveyed the entire physiological landscape (Fig. 2A).

A subtle but important problem in our stochastic simulations was how to decide the timing of cell division. This issue is related to an outstanding question in bacterial physiology: whether replication and division are independently controlled or co-regulated (Koch 1977). We implemented the Helmstetter-Cooper model (Helmstetter and Cooper 1968; Cooper and Helmstetter 1968) that is often interpreted to mean that initiation triggers division after a fixed elapsed time $\tau_{cyc} = C + D$ (Figs. 1A and 2A) (Amir 2014; Amir 2017). To take into account biological stochasticity (Figs. 1C and 2A, Fig. S2A), we allowed for fluctuations in the three physiological variables, three cross-correlations, and three mother/daughter correlations (see Methods). When we incorporated this implicit co-regulation hypothesis and stochasticity

(Amir 2017) in our simulations, we observed that the initiation adder leads to the division adder (Figs. 2B and 2C).

A brute-force numerical investigation of the entire parameter space suggested conditions under which size homeostasis should deviate from adder and, importantly, an experimental means to "break" the adder. Specifically, when we varied the mother-daughter autocorrelation of the initiation size per *ori* s_i away from 0.5, cell-size homeostasis significantly deviated from division adder. Otherwise, most other perturbations to physiological parameters did not severely affect the adder at division, reinforcing the general robustness of adder observed in our inhibition experiments (Fig. 1D). In fact, in the stochastic Helmstetter-Cooper model, the mother-daughter autocorrelation of s_i alone completely determines the initiation adderness (Fig. 2C; Supplemental Information III.A). Since autocorrelation 0.5 is equivalent to exponential convergence of size deviations, modulating the speed of convergence should effectively break adder (Susman *et al*. 2018).

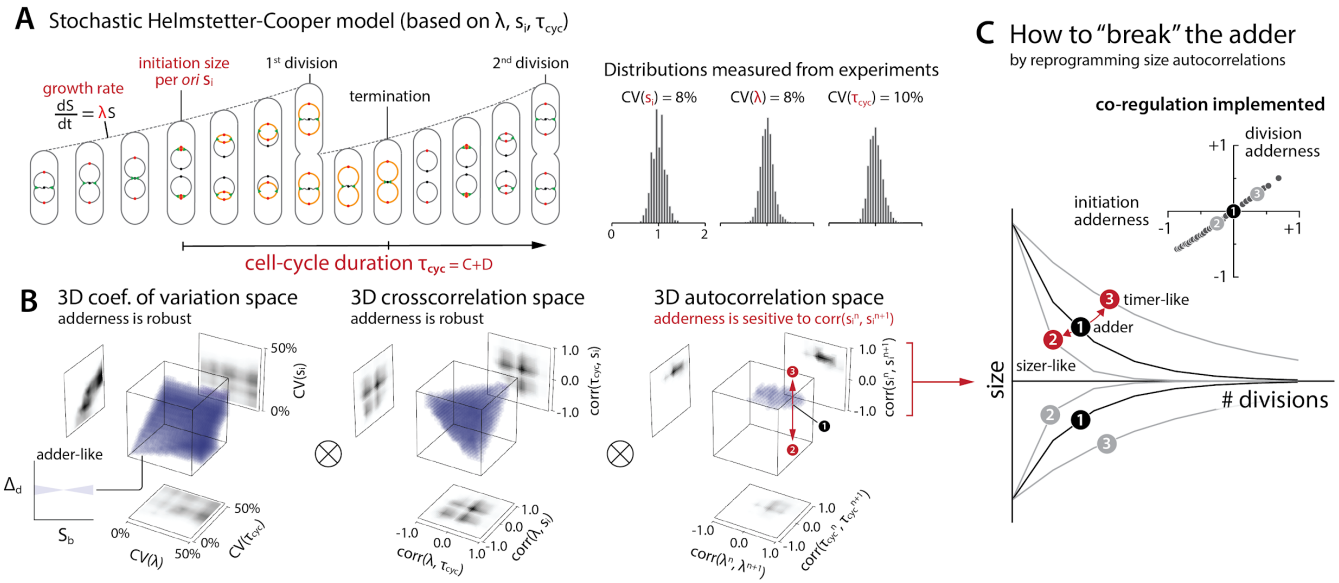

Figure 2: Survey of the 9-dimensional cell-size homeostasis space via stochastic Helmstetter-Cooper model assuming a co-regulation hypothesis between replication initiation and cell division.

(A) The schematics of single-cell simulation. The simulation of cell growth and cell cycle progression took account into the stochasticity of three major physiological variables λ, τ_{cyc}, and s_i measured from experiments. (Methods; Supplemental Information III.A). We did not consider variability in the septum position because it is the least variable physiological parameter in *E. coli* (Taheri-Araghi *et al*. 2014).

(B) The variability of division adderness in the 9-dimensional space surveyed by simulations. Pearson coefficient was used to quantify both cross-correlations (e.g. corr(λ, τ_{cyc})) and mother-daughter autocorrelations (e.g. corr(λ_n , λ_{n+1})). Each 3-D plot is based on 1,000 simulations, and each simulation computed 10,000 division cycles (Supplemental Information III.A). Purple color indicates an adder-like behavior defined as $-0.1 < \mathrm{corr}(\Delta_d , S_b) < 0.1$ (see inset on bottom left). ⊗ means the actual simulation took the convolution of all nine dimensions.

(C) Simulations revealed the unique role of autocorrelation of initiation size per *ori* in determining division adderness. The division adderness corr(Δ_d , S_b) is monotonically dependent on by the initiation adderness corr(δ_i, s_i) when varying the autocorrelation of initiation size per *ori* corr(s_n , s_{n+1}).

Dynamic perturbation to the synthesis of replication initiators breaks the initiation adder

To test our predictions from simulations, we sought to alter the autocorrelation of cell size at initiation in order to modify cell size homeostasis. We found the properties of the DNA replication protein DnaA made it ideal to test our predictions. DnaA is a widely conserved essential protein required for initiation of DNA

replication in bacteria. In bacteria in which it has been examined, replication initiation depends in part on accumulation of a sufficient number of DnaA molecules at the origin of replication (Hansen *et al*. 1991; Skarstad and Katayama 2013; Hansen and Atlung 2018). Previous studies and our data showed that initiation is delayed when DnaA is underexpressed, and an overexpression of DnaA causes premature initiation (Fig. S3A) (Løbner-Olesen *et al*. 1989; Si *et al*. 2017).

To induce negative autocorrelations to initiation size, we periodically modulated synthesis of DnaA (Lin *et al*. 2016) (see Supplemental Information III.C). If the period of oscillation T is two times the doubling time τ, the protein concentration, thus initiation size per *ori*, should be maximally anticorrelated between mother and daughter as illustrated in Fig. 3A. To this end, we adopted a strain encoding an extra copy of *dnaA* with an inducible P_{Lac} promoter and periodically alternated its expression level (Riber *et al*. 2006). We used a period $T \approx 4\tau$ instead of $T = 2\tau$ to take into account the response time of DnaA concentration to induction. Overexpression of DnaA caused over-initiation of chromosome replication (Fig. 3A) without noticeable changes in the growth rate (Fig. S3B). As predicted by our simulations, the measured autocorrelations of initiation size decreased, decisively breaking the initiation adder (Fig. 3A).

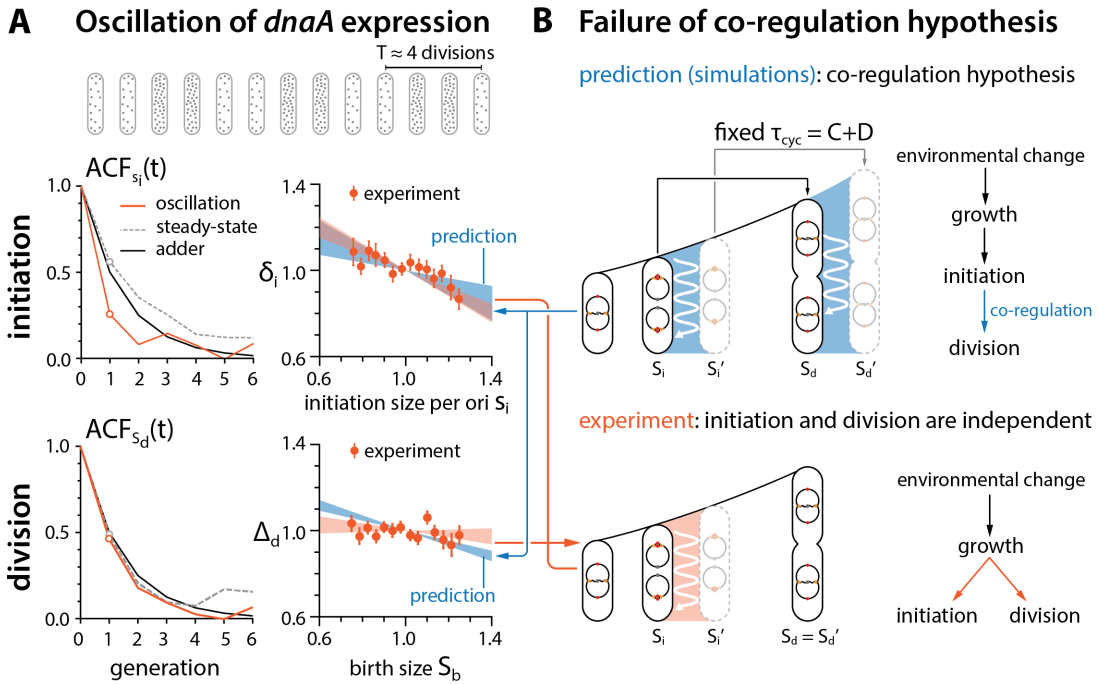

Figure 3: Dynamic perturbation to DnaA production breaks the initiation adder but not the division adder.

(A) Periodic induction of DnaA dynamically modulated initiation size per *ori*, but not division size. This caused deviations in the initiation adder but not in the division adder. The period of the oscillation (T) of the inducer IPTG is about 4τ instead of 2τ considering the actual response time of initiation to DnaA induction (Supplemental Information III.C). The autocorrelation function (ACF) was calculated using Pearson coefficient for each time point. The blue shaded area in the correlation plots represents the prediction from simulations, and the red shaded area indicates the 95% confidence interval of linear fit to the respective raw scatter plot.

(B) The results in (**A**) refutes the co-regulation hypothesis that division timing is determined by initiation timing via a fixed τ_{cyc}. The independence of initiation and division controls warrants a major revision in interpreting the Helmstetter-Cooper model at the single-cell level (Supplemental Information III.B).

The division adder is independent of initiation control, refuting the co-regulation hypothesis

To our surprise, and counter to the co-regulation hypothesis (Amir 2017), the division adder remained intact even when the initiation adder no longer held by periodic induction of DnaA expression (Figs. 3A and 3B). Decoupling between the initiation adder and division adder suggests that the timing of cell division, in fact, has its own independent control (Fig. 3B bottom) (Donachie and Begg 1971; Campos *et al*. 2014; Micali *et al*. 2018a; Micali *et al*. 2018b). We further reasoned that the division timing is regulated by the dynamics of proteins and precursors required *for division*, rather than that of DnaA and other proteins required for replication initiation, and set out to test whether we can break the division adder without breaking the initiation adder.

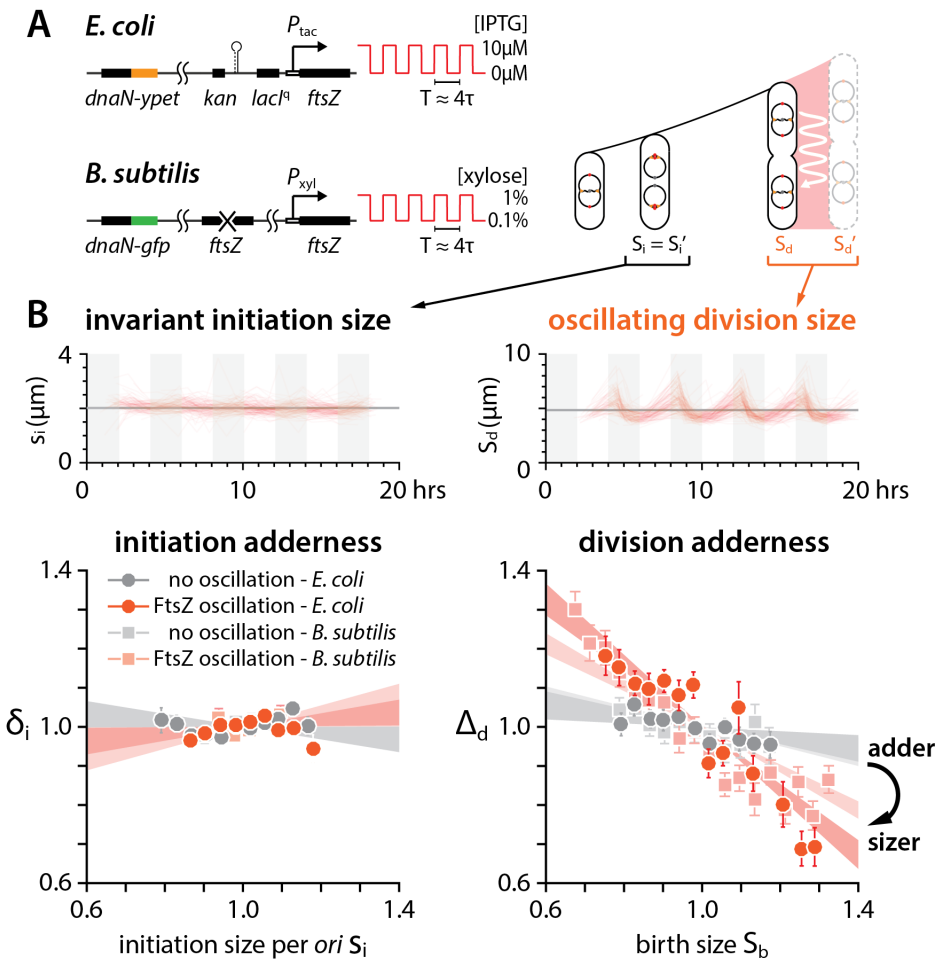

Figure 4: Dynamic perturbation to FtsZ production breaks the division adder but not the initiation adder.

(A) The schematics of genetic modifications for inducible systems of division protein and fluorescence replisome markers. In *E. coli*, the native promoter of *ftsZ* was replaced with a P_{tac} promoter. In *B. subtilis*, the endogenous *ftsZ* was deleted while an alternative copy *ftsZ* under P_{xyl} was inserted at a different loci of the chromosome (see Supplemental Information II.A). Both strains produce fluorescent fusion protein of DnaN for replication tracking. Dynamic modulation of FtsZ was conducted at the oscillation period 4τ, with IPTG concentration oscillating between 0μM and 10 μM for *E. coli*, and Xylose concentration between 0.1% w/v and 1 % w/v for *B. subtilis* (see Fig. S4).

(B) Under FtsZ oscillation, both size homeostasis of *E. coli* and *B. subtilis* become sizer-like, yet their initiation adderness remains intact. In the correlation plots, the variables are normalized by their means and each shaded area represents the 95% confidence interval of linear fit to the respective raw scatter plot.

Dynamic perturbation to the synthesis of division initiators breaks the division adder but not the initiation adder

Cell division requires assembly of more than a dozen types of proteins and biomolecules at the future septum, including the enzymes required for synthesis of the septal cell wall. We elected to use the tubulin-like GTPase, FtsZ because (like DnaA) it is highly conserved and assembles in an expression-level dependent manner. FtsZ-ring formation is required for assembly of all other components of the cell division machinery (Harry *et al*. 2006; Haeusser and Margolin 2016), and the timing of division has been shown to be systematically delayed when FtsZ is underexpressed (Palacios *et al*. 1996; Zheng *et al*. 2016). FtsZ also has practical advantages since its genetic and cytological properties have been extensively characterized (Chien *et al*. 2012).

To determine if oscillations in FtsZ production break the division adder in the same manner that oscillations in DnaA break the initiation adder, we adopted a strain in which the wild-type *ftsZ* was expressed under the control of an inducible promoter (Fig. 4A) (Garrido *et al*. 1993; Palacios *et al*. 1996). We also tracked replication dynamics using the fluorescent replisome marker. When we periodically underexpressed *ftsZ* with a period $T \approx 4\tau$, cell size at division oscillated at the same frequency (Fig. 4B). The mother-daughter correlation of division size significantly deviated from 0.5, and the division adder no longer held. However, the initiation size per *ori* was not affected by the oscillations in division size, and the initiation adder remained intact (Fig. 4B, Figs. S4A and S4C).

We repeated our experiments under different induction levels of *ftsZ* keeping the induction frequency same as before. The degree of deviations from the division adder systematically increased, yet the initiation adder remained intact, underscoring the independence between the initiation adder and the division adder in cell-size homeostasis (Fig. 4B, Figs. S4A and S4C; Supplemental Information III.C). These results also show that cell division processes exclusively drive cell-size homeostasis in *E. coli*.

E. coli and *B. subtilis* likely share the same mechanistic origin of cell-size homeostasis

Next, we asked whether the exclusive role of cell division on size homeostasis, and its independence of initiation control, is a general feature of bacteria. To explore this idea, we repeated the FtsZ oscillation experiments in a model Gram-positive bacterium *B. subtilis*. *B. subtilis* is particularly interesting because, while DnaA and FtsZ are conserved in both bacteria, the mechanisms governing both replication initiation and division in *B. subtilis* differ in fundamental ways from those in *E. coli* (Haeusser and Margolin 2016; Jameson *et al*. 2017). We constructed a strain that encodes *ftsZ* under an inducible P_{xyl} promoter as the sole source of FtsZ, in addition to the functional DnaN-GFP fusion protein (Fig. 4A) (Goranov *et al*. 2009). Together, these constructs permit periodic modulation of FtsZ levels and simultaneous tracking of replication dynamics.

Similar to *E. coli*, *B. subtilis* exhibited systematic deviations from the division adder when *ftsZ* expression was varied periodically. Furthermore, we found *B. subtilis* to be an initiation adder regardless of the oscillations (Fig. 4B, Figs. S4B and S4D). These results strongly suggested that *E. coli* and *B. subtilis* share the same mechanistic origin of cell-size homeostasis.

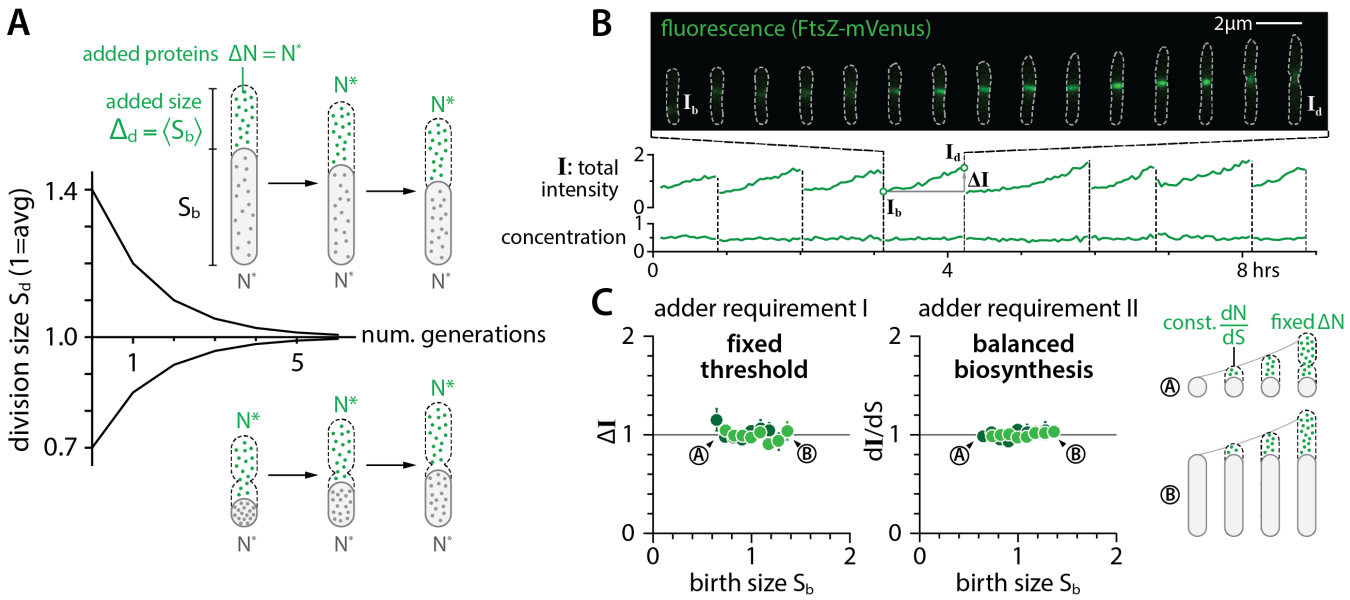

Figure 5: The mechanistic origin of the adder.

(A) The adder phenotype requires accumulation of division proteins to a fixed amount 2N* to trigger division, and their balanced biosynthesis during growth. Under these conditions, newborn cells are born either larger or smaller than the population average, but they on average contain N* division proteins. The two adder requirements ensure that both small-born and large-born cells add a constant size (or N* division proteins) in each generation.

(B) A typical timelapse sequence with FtsZ-mVenus. The total intensity was obtained by integrating the FtsZ-mVenus fluorescence intensity over the entire cell, which increases steadily from birth to division, tracking the total size of the cell. As a result, the FtsZ-mVenus concentration stays nearly constant within fluctuations.

(C) The synthesis and accumulation of FtsZ in *E. coli* cells fulfills both requirements for adder. The total added number ΔN (estimated by the added fluorescence ΔI) and the synthesis per unit volume dN/dS were constant and independent of cell size at birth (see Fig. S5). Symbol colors indicate repeats of experiments.

Mechanistic origin of cell-size homeostasis in bacteria: threshold and balanced biosynthesis

Our data so far indicated it is possible to break the adder phenotype using periodic oscillations in the production rate of cell-cycle proteins to perturb initiation size or division size (DnaA for the initiation adder and FtsZ for the division adder). This finding suggests that balanced biosynthesis of cell-cycle proteins is likely an important requirement for the adder phenotype.

In balanced biosynthesis, the protein production rate is proportional to the rate cells increase their volume, irrespective of the protein concentration at birth. The total number of newly synthesized proteins is therefore directly proportional to the total cell volume added since birth.

Assuming balanced biosynthesis, a cell would be a division adder if division is triggered at a fixed volume after accumulating a fixed number of division proteins (Fig. 5A). In other words, two experimentally supported assumptions are sufficient to explain the adder phenotype: (1) Threshold -- accumulation of initiators and precursors required for cell division to a respective fixed number, and (2) Balanced biosynthesis -- maintenance of their production proportional to volume growth.

To test this idea, we measured the production rate and the accumulation of FtsZ in single cells. We adopted an *E. coli* strain expressing a nearly functional fusion *ftsZ*-mVenus as the sole endogenous copy of *ftsZ* (Moore *et al*. 2017). We used the total fluorescence per cell to estimate the total copy number of FtsZ per cell (Fig. 5B; Methods). During steady-state growth, the total FtsZ-mVenus intensity increased

proportionally to the increase in volume in individual cells (Fig. S5B). The production of FtsZ-mVenus per unit volume during growth was independent of the cell size or FtsZ concentration at birth, consistent with the balanced biosynthesis hypothesis (Fig. 5C; Fig. S5C) (Sigal *et al*. 2016; Jajoo *et al*. 2016). Furthermore, the total accumulation of FtsZ-mVenus until division was also constant and independent of cell size or FtsZ concentration at birth, supporting the threshold hypothesis (Fig. 5C; Fig. S5C) (Teather *et al*. 1974; Bi and Lutkenhaus 1990; Basan *et al*. 2015; Harris and Theriot 2016; Ghusinga *et al*. 2016). As explained below, we further verified these hypotheses in our oscillation experiments.

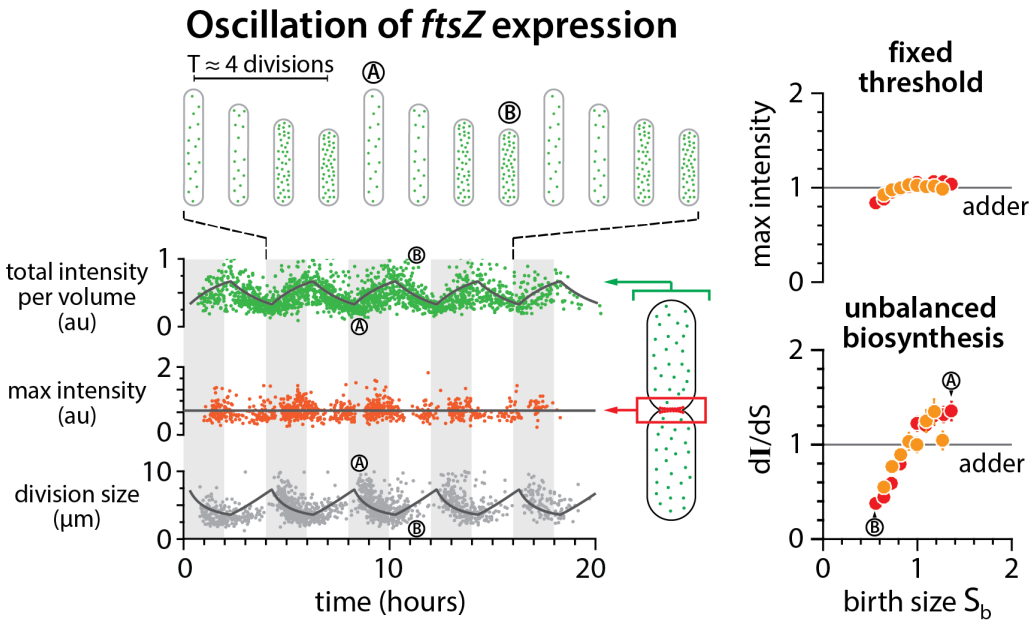

Figure 6: Testing the mechanism of adder in the FtsZ oscillation experiment.

Left: Total FtsZ-mVenus concentration oscillates in response to the periodic induction, but the threshold amount at the septum is invariant. The amount of FtsZ accumulated in the septum ring was estimated by integrating the fluorescence intensity within a fixed area enclosing the mid-cell region (Methods; Supplemental Information II.D; Fig. S5).

Right: Despite the oscillations in the total FtsZ concentration, the max Z-ring intensity remains invariant with respect to birth size. In contrast, the production rate of FtsZ was variable due to oscillations (see Supplemental Information III.C for the prediction of dI/dS vs. S_b). Symbol colors indicate repeats of experiments.

Testing the mechanism of the adder in the FtsZ oscillation experiments

As the steady-state growth experiments supported the threshold and balanced biosynthesis hypotheses, we further tested them to explain how the adder breaks in the oscillation experiments. We replaced the native promoter of *ftsZ-mVenus* with an inducible promoter allowing us to periodically express *ftsZ-mVenus* and directly quantify FtsZ concentration (Moore *et al*. 2017) (Fig. S6A; Supplemental Information II.A). As expected, FtsZ-mVenus concentration oscillated in response to the periodic induction, while the division size exhibited clear out-of-phase oscillations (Fig. 6 left; Supplemental Information III.C).

To verify the threshold hypothesis, we measured the fluorescence intensity of FtsZ-mVenus at mid-cell as a proxy for FtsZ concentration at septum (Fig. 6 left, Fig. S5A). As previously reported Z-ring appeared at mid-cell shortly after birth and FtsZ-mVenus intensity at this site steadily increased over the course of the division cycle (van der Ploeg *et al*. 2013; Söderström *et al*. 2014; Coltharp *et al*. 2016) (Fig. 5B, Fig. S5A). Total Z-ring intensity reached its max value at the late stage of division cycle, coinciding with the

onset of cell constriction. Despite the oscillations in FtsZ-mVenus concentration, the maximal Z-ring intensity at mid-cell remained remarkably constant throughout the experiments regardless of the FtsZ concentration or cell size at birth (Fig. 6 left; Fig. S6C).

The sizer-like behavior can also be explained by the out-of-phase oscillations in the FtsZ concentration and division size. During periodic induction of *ftsZ*, small-born daughter cells contain higher concentrations of FtsZ, because their mother cells accumulated FtsZ at a faster rate during high-level induction and therefore divided early. These new small-born daughter cells in turn experience low-level induction (Fig. 6 bottom right), thus accumulate FtsZ to the fixed threshold number at a slower-rate and elongate longer to reach division (Fig. 6 top right). In other words, small-born cells add a larger size until division, whereas large-born cells add a smaller size until division, which is the behavior of a sizer. Indeed, the added size Δ_d vs. newborn size s_b shows a characteristic sizer-like negative slope (Fig. S6C; Fig. 4).

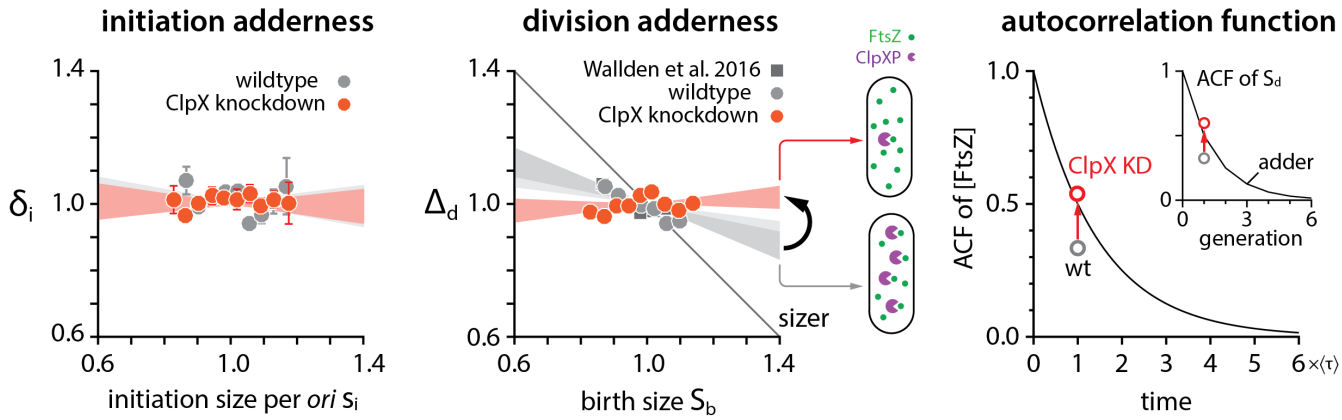

Figure 7: Restoring the division adder.

Left: Slow growing E. coli cells are initiation adders (this work) but not division adders (this work and Wallden *et al*. 2016; the doubling time was about 4 hours). Repressing *clpX* expression via tCRISPRi restored the division adder. Each shaded area represents the 95% confidence interval of linear fit to the respective raw scatter plot.

Right: The mother-daughter autocorrelation of division size was less than 0.5 in slow growing cells, indicating a more sizer-like behavior. The autocorrelation function of FtsZ concentration was also less than 0.5. The repression of *clpX* expression alleviated both deviations (see Supplemental Information II.C).

How to restore the adder phenotype in slow-growing *E. coli*

While a wide range of evolutionarily divergent organisms are adders (Jun *et al*. 2018), a major exception has also been reported for *E. coli*. Specifically, Wallden e*t al*. reported that size homeostasis, during slow growth in nutrient limitation, deviates from the adder (Wallden *et al*. 2016). We re-analyzed the published data in Wallden *et al*. and also performed our own experiments in the same growth conditions. In contrast to Wallden *et al*., we found that the slope in the Δ_d vs. newborn size s_b is in fact much closer to the adder (slope = 0) than the sizer (slope = -1) in both experiments. At the same time, the deviations from the adder is statistically significant (p-value = 1.4×10^{-6}) as pointed out by Wallden *et al*.

Wallden *et al*. provided a possible explanation for their observation, based on the Helmstetter-Cooper model at the single-cell level. That is, the cell size at division can be written as $S_d = s_i\exp(\tau_{cyc}/\tau)$ when τ_{cyc} is shorter than τ in slow growing cells. If s_i is invariant while τ_{cyc} increases proportionally to τ at the single cell level (Wallden *et al*. 2016), τ_{cyc}/τ = constant and therefore the invariant s_i implies S_d is fixed regardless of the birth size, thus the sizer.

While elegant, this explanation is based on the co-regulation hypothesis and would have predicted both slope in Δ_d vs. s_b and Δ_i vs. s_i to be -1. However, our data showed that slow growing *E. coli* is an initiation adder, and the division adderness is -0.22 instead of -1 (Fig. 7 left). For the above explanation to be valid, both τ_{cyc}/τ and s_i should be uncorrelated with birth size, which is in conflict with our data (Fig. S7A).

Reasoning that the slow-growing *E. coli* violates one or both conditions for the division adder (Fig. 5), we sought to clarify the discrepancy between our finding and the conclusion of Wallden *et al*.. Specifically, we predicted that it would be balanced biosynthesis of division proteins, rather than their threshold, that is likely affected by the slow growth conditions. This view was also consistent with recent reports that FtsZ is likely actively degraded by the ClpXP protease complex in slow growth conditions (Sekar *et al*. 2018; Männik *et al*. 2018). If FtsZ is actively degraded, the turnover rate of FtsZ should increase so that both autocorrelation of FtsZ concentration and division size should decrease (Fig. 7 right; see the modeling with stochasticity in Supplemental Information III.A). This would impair the balanced biosynthesis (Fig. S7B), and the size homeostasis should deviate towards a sizer (Methods). This intuition can be quantitatively formulated, and we show that the pattern of cell-size homeostasis becomes more sizer-like when division proteins are actively degraded (see Methods).

We tested our prediction by represseding *clpX* expression using our tCRISPRi (Li *et al*. 2016). We found that the *clpX* repression was indeed sufficient to fully restore the division adder. The initiation adder was intact with or without the *clpX* repression (Fig. 7). These results provide strong experimental evidence for balanced biosynthesis and threshold as the requirements for cell-size homeostasis to be an adder.

Relationship with previous works

Balanced biosynthesis and threshold are general concepts in biology and have been implied in a number of papers since the 1970s from replication initiation (Sompayrac and Maaløe 1973) or cell division (Taheri-Araghi *et al*. 2014; Basan *et al*. 2015; Ghusinga *et al*. 2016) in bacteria to mitotic control in eukaryotes (Fantes *et al*. 1975). The threshold model has also been explicitly put forward as the trigger of cell division as starved *E. coli* cells resume growth (Sekar *et al*. 2018). A recent work addressed whether cell shape contributes to size control (Harris and Theriot 2016), but we recognize its core implicit assumptions are balanced biosynthesis of cell-wall precursors and their accumulation to a threshold to build the septum.

Previous work independently showed that *E. coli* is a division adder but also questioned whether size control is implemented at initiation or division (Campos *et al*. 2014). We have shown that division drives size homeostasis in *E. coli* and *B. subtilis*, but they are both initiation and division adders in steady state (Fig. 1D). The independence between the two types of adders can only be revealed in non steady-state growth (Figs. 3 and 4). Subsequent analysis (Ho and Amir 2015) has shown that the experimental evidence in Campos *et al*. may in fact agree with the initiation adder. As we show in Supplemental Information IV.B, the initiation control model in (Campos *et al*. 2014) can result in unstable cell size regulation, but can be corrected when growth by a constant size *per origin* is implemented at initiation in steady-state growth (see Supplemental Information IV.B).

Another notable proposal for cell-size control in *E. coli* is a negative feedback imposed on cell size (Tanouchi *et al*. 2015). The hypothetical feedback exclusively relied on transient "oscillations" observed in the autocorrelation function (ACF) of cell size in experimental data and simulation data of an

autoregressive model. However, it is well known that the ACF of the autoregressive model they used is an exponential function, in contradiction with the claimed oscillations. In other words, it is likely that the "oscillations" observed in both experimental and simulation ACFs are fortuitous, and caused by an insufficient sampling (approximately N=70 generations in each lineage) that fails to produce statistically meaningful autocorrelation coefficients.

CONCLUSION AND OUTLOOK

Altogether, we have shown that it is cell division (Campos *et al*. 2014; Basan *et al*. 2015; Harris and Theriot 2016; Taheri-Araghi *et al*. 2014), not replication initiation (Amir 2014; Ho and Amir 2015; Amir 2017), that drives cell-size homeostasis in bacteria. Initiation control is important in cell-size control, rather than cell-size homeostasis, because initiation defines unit cellular volume (or "unit cell") so that the average cell size in any steady-state population is given by the sum of all unit cells (Si *et al*. 2017). From the cell-cycle control point of view, we showed that initiation and division are independently controlled in both *E. coli* and *B. subtilis*, thereby providing a conclusive answer to the long-standing question whether replication initiation regulates cell division in bacteria (Koch 1977).

The mechanism underlying the adder phenotype for size homeostasis reduces to two biological hypotheses: (1) balanced biosynthesis of division proteins and precursors and (2) their accumulation to a threshold number in individual cells. In this work, we provided direct experimental evidence that support these two hypotheses for cell-size control and homeostasis. In our view, a next major question for the future is how a threshold model is implemented at the molecular level in division control and the cell cycle control in general, while continuing a constructive dialog between quantitative phenomenological principles and mechanistic investigation.

The mechanism of adder has obvious implications on its applicability to other biological problems such as homeostasis of organelle content (Jajoo *et al*. 2016). From an evolutionary point of view, cell-cycle dependent degradation of cyclins may explain why some eukaryotes show clear departure from adder by actively modulating physiological memory. But perhaps a more curious case is the mechanism of size homeostasis of the First Cells or synthetic cells, for which the simplicity of balanced growth makes adder an intriguing possibility.

REFERENCES

1. Adiciptaningrum, A., Osella, M., Moolman, M. C., Lagomarsino, M. C., and Tans, S. J. (2015). Stochasticity and homeostasis in the *E. coli* replication and division cycle. *Scientific Reports*, 5(1):18261.

2. Amir, A. (2014). Cell size regulation in bacteria. *Physical Review Letters*, 112(20):208102.

3. Amir, A. (2017). Is cell size a spandrel? *eLife*, 6:e22186.

4. Basan, M., Zhu, M., Dai, X., Warren, M., Sévin, D., Wang, Y. P., and Hwa, T. (2015). Inflating bacterial cells by increased protein synthesis. *Molecular Systems Biology*, 11(10):836.

5. Bertaux, F., Kügelgen, J. V., Marguerat, S., and Shahrezaei, V. (2016). A unified coarse- grained theory of bacterial physiology explains the relationship between cell size, growth rate and proteome composition under various growth limitations. *bioRxiv*, page 078998.

6. Bi, E. and Lutkenhaus, J. (1990). FtsZ regulates frequency of cell division in *Escherichia coli*. *Journal of bacteriology*, 172(5):2765–8.

7. Cadart, C., Monnier, S., Grilli, J., Sáez, P. J., Srivastava, N., Attia, R., Terriac, E., Baum, B., Cosentino-Lagomarsino, M., and Piel, M. (2018). Size control in mammalian cells involves modulation of both growth rate and cell cycle duration. *Nature Communications*, 9(1):3275.

8. Campos, M., Surovtsev, I. V., Kato, S., Paintdakhi, A., Beltran, B., Ebmeier, S. E., and Jacobs-Wagner, C. (2014). A constant size extension drives bacterial cell size homeostasis. *Cell*, 159(6):1433–1446.

9. Chandler-Brown, D., Schmoller, K. M., Winetraub, Y., and Skotheim, J. M. (2017). The adder phenomenon emerges from independent control of pre- and post-start phases of the budding yeast cell cycle. *Current Biology*.

10. Chien, A.-C., Hill, N. S., and Levin, P. A. (2012). Cell size control in bacteria. *Current Biology*, 22(9):R340–R349.

11. Coltharp, C., Buss, J., Plumer, T. M., and Xiao, J. (2016). Defining the rate-limiting processes of bacterial cytokinesis. *Proceedings of the National Academy of Sciences*, 113(8):E1044–E1053.

12. Cooper, S. and Helmstetter, C. E. (1968). Chromosome replication and the division cycle of *Escherichia coli* B/r. *Journal of Molecular Biology*, 31(3):519–540.

13. Cox, S., Rosten, E., Monypenny, J., Jovanovic-Talisman, T., Burnette, D. T., Lippincott- Schwartz, J., Jones, G. E., and Heintzmann, R. (2011). Bayesian localization microscopy reveals nanoscale podosome dynamics. *Nature Methods*, 9(2):195–200.

14. Deforet, M., Van Ditmarsch, D., and Xavier, J. B. (2015). Cell-size homeostasis and the incremental rule in a bacterial pathogen. *Biophysical Journal*, 109(3):521–528.

15. Donachie, W. D. (1968). Relationship between Cell Size and Time of Initiation of DNA Replication. *Nature*, 219(5158):1077-1079.

16. Donachie, W. D., and Begg, M. K. J. (1971). Independence of Cell Division and DNA Replication in *Bacillus subtilis*. *Nature*, 231(26):274-276.

17. Fantes, P. A., Grant, W. D., Pritchard, R. H., Sudbery, P. E., and Wheals, A. E. (1975). The regulation of cell size and the control of mitosis. *Journal of Theoretical Biology*, 50(1):213–244.

18. Garrido, T., Sánchez, M., Palacios, P., Aldea, M., and Vicente, M. (1993). Transcription of FtsZ oscillates during the cell cycle of *Escherichia coli*. *The EMBO journal*, 12(10):3957–65.

19. Ghusinga, K. R., Vargas-Garcia, C. A., and Singh, A. (2016). A mechanistic stochastic framework for regulating bacterial cell division. *Scientific Reports*, 6(1):30229.

20. Goranov, A. I., Breier, A. M., Merrikh, H., and Grossman, A. D. (2009). YabA of *Bacillus subtilis* controls DnaA-mediated replication initiation but not the transcriptional response to replication stress. *Molecular Microbiology*, 74(2):454–466.

21. Haeusser, D. P. and Margolin, W. (2016). Splitsville: structural and functional insights into the dynamic bacterial Z ring. *Nature Reviews Microbiology*, 14(5):nrmicro.2016.26.

22. Hansen, F. G. and Atlung, T. (2018). The DnaA tale. *Frontiers in Microbiology*, 9:319. Hansen, F. G., Atlung, T., Braun, R. E., Wright, A., Hughes, P., and Kohiyama, M. (1991).

23. Initiator (DnaA) protein concentration as a function of growth rate in *Escherichia coli* and *Salmonella typhimurium*. *Journal of bacteriology*, 173(16):5194–9.

24. Harris, L. K. and Theriot, J. A. (2016). Relative rates of surface and volume synthesis set bacterial cell size. *Cell*, 165(6):1479–1492.

25. Harry, E., Monahan, L., and Thompson, L. (2006). Bacterial cell division: the mechanism and its precision. *International review of cytology*, 253:27–94.

26. Helmstetter, C. E. and Cooper, S. (1968). DNA synthesis during the division cycle of rapidly growing *Escherichia coli* B/r. *Journal of Molecular Biology*, 31(3):507–518.

27. Ho, P.-Y. and Amir, A. (2015). Simultaneous regulation of cell size and chromosome replication in bacteria. *Frontiers in Microbiology*, 6:662.

28. Holden, S. J., Uphoff, S., and Kapanidis, A. N. (2011). Daostorm: an algorithm for high-density super-resolution microscopy. *Nature Methods*, 8(4):279–280.

29. Iyer-Biswas, S., Wright, C. S., Henry, J. T., Lo, K., Burov, S., Lin, Y., Crooks, G. E., Crosson, S., Dinner, A. R., and Scherer, N. F. (2014). Scaling laws governing stochastic growth and division of single bacterial cells. *Proceedings of the National Academy of Sciences*, 111(45):15912–15917.

30. Jajoo, R., Jung, Y., Huh, D., Viana, M. P., Rafelski, S. M., Springer, M., and Paulsson, J. (2016). Accurate concentration control of mitochondria and nucleoids. *Science*, 351(6269):169–172.

31. Jameson, K. H. and Wilkinson, A. J. (2017). Control of initiation of DNA replication in *Bacillus subtilis* and *Escherichia coli*. *Genes*, 8(1):22.

32. Jun, S., Si, F., Pugatch, R., and Scott, M. (2018). Fundamental principles in bacterial physiology - history, recent progress, and the future with focus on cell size control: A review. *Reports on progress in physics. Physical Society (Great Britain)*.

33. Jun, S. and Taheri-Araghi, S. (2015). Cell-size maintenance: universal strategy revealed. *Trends in Microbiology*, 23(1):4–6.

34. Kiviet, D. J., Nghe, P., Walker, N., Boulineau, S., Sunderlikova, V., and Tans, S. J. (2014). Stochasticity of metabolism and growth at the single-cell level. *Nature*, 514(7522):nature13582.

35. Koch, A. L. (1977). Does the initiation of chromosome replication regulate cell division? In *Advances in microbial physiology*, volume 16, pages 49–98. Elsevier.

36. Li, X.-T., Jun, Y., Erickstad, M. J., Brown, S. D., Parks, A., Court, D. L., and Jun, S. (2016). tCRISPRi: tunable and reversible, one-step control of gene expression. *Scientific Reports*, 6(1):39076.

37. Lin, W.-H. and Kussell, E. (2016). Complex interplay of physiology and selection in the emergence of antibiotic resistance. *Current Biology*, 26(11):1486–1493.

38. Løbner-Olesen, A., Skarstad, K., Hansen, F. G., Meyenburg, K. V., and Boye, E. (1989). The DnaA protein determines the initiation mass of *Escherichia coli* K-12. *Cell*, 57(5):881–889.

39. Logsdon, M. M., Ho, P.-Y., Papavinasasundaram, K., Richardson, K., Cokol, M., Sassetti, C. M., Amir, A., and Aldridge, B. B. (2017). A parallel adder coordinates mycobacterial cell-cycle progression and cell-size homeostasis in the context of asymmetric growth and organization. *Current Biology*, 27(21):3367–3374.e7.

40. Mangiameli, S. M., Veit, B. T., Merrikh, H., and Wiggins, P. A. (2017). The replisomes remain spatially proximal throughout the cell cycle in bacteria. *PLOS Genetics*, 13(1):e1006582.

41. Männik, J., Walker, B. E., and Männik, J. (2018). Cell cycle-dependent regulation of FtsZ in *Escherichia coli* in slow growth conditions. *Molecular Microbiology*.

42. Micali, G., Grilli, J., Marchi, J., Osella, M., and Lagomarsino, M. C. (2018a). Dissecting the control mechanisms for DNA replication and cell division in *E. coli*. *Cell Reports*, 25(3):761–771.e4.

43. Micali, G., Grilli, J., Osella, M., and Lagomarsino, M. C. (2018b). Concurrent processes set *E. coli* cell division. *Science Advances*, 4(11):eaau3324.

44. Moore, D. A., Whatley, Z. N., Joshi, C. P., Osawa, M., and Erickson, H. P. (2017). Probing for binding regions of the FtsZ protein surface through site-directed insertions: Discovery of fully functional FtsZ-fluorescent proteins. *Journal of bacteriology*, 199(1):e00553–16.

45. Osella, M., Nugent, E., and Lagomarsino, M. C. (2014). Concerted control of *Escherichia coli* cell division. *Proceedings of the National Academy of Sciences*, 111(9):3431–3435.

46. Palacios, P., Vicente, M., and Sánchez, M. (1996). Dependency of *Escherichia coli* cell- division size, and independency of nucleoid segregation on the mode and level of FtsZ expression. *Molecular Microbiology*, 20(5):1093–1098.

47. Ploeg, R. V. D., Verheul, J., Vischer, N. O. E., Alexeeva, S., Hoogendoorn, E., Postma, M., Banzhaf, M., Vollmer, W., and Blaauwen, T. (2013). Colocalization and interaction between elongasome and divisome during a preparative cell division phase in *Escherichia coli*. *Molecular Microbiology*, 87(5):1074–1087.

48. Riber, L., Olsson, J. A., Jensen, R. B., Skovgaard, O., Dasgupta, S., Marinus, M. G., and Løbner-Olesen, A. (2006). Hda-mediated inactivation of the DnaA protein and DnaA gene autoregulation act in concert to ensure homeostatic maintenance of the *Escherichia coli* chromosome. *Genes & Development*, 20(15):2121–2134.

49. Santi, I., Dhar, N., Bousbaine, D., Wakamoto, Y., and Mckinney, J. D. (2013). Single- cell dynamics of the chromosome replication and cell division cycles in mycobacteria. *Nature Communications*, 4:2470.

50. Sauls, J. T., Li, D., and Jun, S. (2016). Adder and a coarse-grained approach to cell size homeostasis in bacteria. *Current Opinion in Cell Biology*, 38:38–44.

51. Schaechter, M., Maaløe, O., and Kjeldgaard, N. O. (1958). Dependency on medium and temperature of cell size and chemical composition during balanced growth of *Salmonella typhimurium*. *Journal of General Microbiology*, 19(3):592–606.

52. Sekar, K., Rusconi, R., Sauls, J. T., Fuhrer, T., Noor, E., Nguyen, J., Fernandez, V. I., Buffing, M. F., Berney, M., Jun, S., Stocker, R., and Sauer, U. (2018). Synthesis and degradation of FtsZ quantitatively predict the first cell division in starved bacteria. *Molecular Systems Biology*, 14(11):e8623.

53. Si, F., Li, D., Cox, S. E., Sauls, J. T., Azizi, O., Sou, C., Schwartz, A. B., Erickstad, M. J., Jun, Y., Li, X., and Jun, S. (2017). Invariance of initiation mass and predictability of cell size in *Escherichia coli*. *Current Biology*, page 081422.

54. Sigal, A., Milo, R., Cohen, A., Geva-Zatorsky, N., Klein, Y., Liron, Y., Rosenfeld, N., Danon, T., Perzov, N., and Alon, U. (2006). Variability and memory of protein levels in human cells. *Nature*, 444(7119):643–646.

55. Skarstad, K. and Katayama, T. (2013). Regulating DNA replication in bacteria. *Cold Spring Harbor Perspectives in Biology*, 5(4):a012922.

56. Söderström, B., Skoog, K., Blom, H., Weiss, D. S., Heijne, G., and Daley, D. O. (2014). Disassembly of the divisome in *Escherichia coli*: evidence that FtsZ dissociates before compartmentalization. *Molecular Microbiology*, 92(1):1–9.

57. Soifer, I., Robert, L., and Amir, A. (2016). Single-cell analysis of growth in budding yeast and bacteria reveals a common size regulation strategy. *Current Biology*, 26(3):356–361.

58. Sompayrac, L. and Maaløe, O. (1973). Autorepressor model for control of DNA replication. *Nature*, 241(109):133–135.

59. Susman, L., Kohram, M., Vashistha, H., Nechleba, J. T., Salman, H., and Brenner, N. (2018). Individuality and slow dynamics in bacterial growth homeostasis. *Proceedings of the National Academy of Sciences*, 115(25):201615526.

60. Taheri-Araghi, S., Bradde, S., Sauls, J. T., Hill, N. S., Levin, P. A., Paulsson, J., Vergassola, M., and Jun, S. (2015). Cell-size control and homeostasis in bacteria. *Current Biology*, 25(3):385–391.

61. Talia, S. D., Skotheim, J. M., Bean, J. M., Siggia, E. D., and Cross, F. R. (2007). The effects of molecular noise and size control on variability in the budding yeast cell cycle. *Nature*, 448:947–951.

62. Tanouchi, Y., Pai, A., Park, H., Huang, S., Stamatov, R., Buchler, N. E., and You, L. (2015). A noisy linear map underlies oscillations in cell size and gene expression in bacteria. *Nature*, 523(7560):357–360.

63. Teather, R. M., Collins, J. F., and Donachie, W. D. (1974). Quantal behavior of a diffusible factor which initiates septum formation at potential division sites in *Escherichia coli*. *Journal of bacteriology*, 118(2):407–13.

64. Varsano, G., Wang, Y., and Wu, M. (2017). Probing mammalian cell size homeostasis by channel-assisted cell reshaping. *Cell Reports*, 20(2):397–410.

65. Wallden, M., Fange, D., Lundius, E. G., Baltekin, ö., and Elf, J. (2016). The synchronization of replication and division cycles in individual *E. coli* cells. *Cell*, 166(3):729–739.

66. Wang, P., Robert, L., Pelletier, J., Dang, W. L., Taddei, F., Wright, A., and Jun, S. (2010). Robust growth of *Escherichia coli*. *Current Biology*, 20(12):1099–1103.

67. Willis, L. and Huang, K. C. (2017). Sizing up the bacterial cell cycle. *Nature Reviews Microbiology*.

68. Zheng, H., Ho, P.-Y., Jiang, M., Tang, B., Liu, W., Li, D., Yu, X., Kleckner, N. E., Amir, A., and Liu, C. (2016). Interrogating the *Escherichia coli* cell cycle by cell dimension perturbations. *Proceedings of the National Academy of Sciences*, 113(52):15000–15005.

METHODS

Strain and growth conditions. *E. coli* strains used in this study are with background of either K-12 NCM3722 or K-12 MG1655. *B. subtilis* strains used here were constructed based on the JH642 background. See detailed information of strain construction in Supplemental Information II.A. Defined media were used in all experiments. For *E. coli*, we used MOPS or M9 minimal media supplied with different carbon sources and amino acids. For *B. subtilis*, S750 minimal media with different carbon sources and other supplements were used. See detailed information of growth media in Supplemental Information II.B.

Microfluidics. Mother machine microfluidic devices were used in this study to monitor single cell growth for 10-50 generations in both steady state and oscillation experiments. Syringe pumps (PHD Ultra, Harvard Apparatus, MA) were programmed to infuse fresh growth media into microfluidic device at either constant rate or in an oscillatory manner.

Cell preparation. Before every time-lapse imaging, cells were picked from a single colony on an agar plate which was streaked no more than 7 days before use. The cells were inoculated into 1 mL lysogeny broth (LB) with proper selection antibiotics. After shaken for 12-18 hours at 30 °C or 37 °C water bath shaker, cells were diluted 1,000-fold into 2 mL of defined medium same as that used in microfluidic experiment. After shaken at 37 °C in water bath till OD600 = 0.1-0.4, cells were diluted again 100- to 1,000-fold into the same medium and shaken at 37 °C in water bath till OD600 = 0.1-0.4. The cell culture was then concentrated 10- to 100-fold and injected into a microfluidic mother machine device via a 1 mL syringe. 0.5 mg mL^{-1} BSA (Bovine serum albumin, Gemini Bio Products, CA) was added to the fresh growth media to reduce the adhesion of cells to the surface of microfluidic channels. The media were then added to 10 mL, 20 mL or 60 mL plastic syringes (BD) with 0.22 μm filters (Genesee Scientific, CA) for the time-lapse imaging. All imaging experiments were conducted at 37 °C in an environmental chamber[3].

Microscopy and image acquisition. We performed simultaneous phase-contrast and epifluorescence imaging on an inverted microscope (Nikon Ti-E) with Perfect Focus 3 (PFS3), 100x oil immersion objective (PH3, numerical aperture = 1.45), Obis lasers 488LX or 561LS (Coherent Inc., CA) as fluorescence light source, and Andor NEO sCMOS (Andor Technology) or Prime 95B sCMOS camera (Photometrics). The laser power was 18 mW for 488 nm excitation and 17 mW for 561 nm, respectively. Exposure time was set between 50-200 ms. Imaging frequency were calibrated at about 20 frames per doubling time such that no physiological effects on the cells were discernible.

Image processing. Time lapse images were processed using custom software written in Python and Matlab (Mathworks Inc.). Specifically, phase-contrast images of cells were used for cell segmentation, lineage reconstruction and cell dimension measurement. See details in Supplemental Information II.D. Fluorescence images of replisome markers were used to quantify the cell cycle of single cells. Fluorescence foci were identified as local maxima using a Laplacian of Gaussian method. The distribution of all foci intensity was fitted with a double Gaussian function and used for intensity weighting which corrects the foci number per cell, with the position of the second peak approximately two times that of the first (Fig. 1B). Intracellular positions of all foci in the same cells were plotted against time for the whole single lineage. The start and end points of each foci trace were determined as the replication initiation and termination with respect to division cycles (Fig. S1). See more details in Supplemental Information II.D.

Fluorescence images of FtsZ-mVenus were used to estimate the total amount FtsZ per cell, the total concentration of FtsZ, the total fluorescence of the Z-ring and the cytoplasmic concentration of FtsZ. The first 5-10 generations of the time-lapse images were discarded to ensure that photobleaching reaches stationarity of the timelapse data. The total fluorescence of FtsZ per cell was used to estimate the total amount FtsZ per cell. The total fluorescence normalized by cell volume was used to estimate the total concentration of FtsZ. The amount of FtsZ in the mid-cell area was quantified by integrating the fluorescence intensity within a fixed box with dimensions of 1 μm along cell long-axis and 1.5x cell width along short axis. This area is centered at max intensity position of the line profile along cell long-axis. This quantity was used as an approximation of the total fluorescence in the Z-ring. The cytoplasmic concentration of FtsZ was estimated as the total fluorescence within an area of the same size centered at a cell-quarter position along the cell long-axis. See more details in Supplemental Information II.D.

Stochastic simulations of the Helmstetter-Cooper model. To investigate what determines cell-size homeostasis we developed stochastic simulations of the Helmstetter-Cooper cell cycle model[17]. In this model, three coarse-grained physiological parameters describe the progression of the cell cycle and cell size: the growth rate λ, the cell size at initiation per origin s_i , and the length of cell cycle $\tau_{cyc} = C+D$, namely the duration that spans one complete round of replication (C period) and division that corresponds to replication termination (D period). We introduced stochasticity to these parameters (λ, s_i , τ_{cyc}) and numerically probed the resulting behavior of cell-size homeostasis (Fig. 1C). See more details in Supplemental Information III.A. The stochastic fluctuations constituted a 9-dimensional physiological space consisting of three autocorrelations, three cross-correlations, and three coefficient-of-variations (CVs) (Fig. 2A), with each physiological dimension representing specific biological constraints. For instance, positive autocorrelations in the growth rate λ mean that on average fast-growing mother cells produce fast-growing daughter cells. When these refinements were added, our stochastic simulations self-consistently reproduced the experimentally observed adder behavior for all tested growth conditions without any adjustable parameters (Supplemental Information III.A). In Fig. 2A, we set out to systematically vary physiological parameters along all nine dimensions to probe the adder behavior. Each simulation generated a lineage of 10,000 cells. The adder correlation $\rho(\Delta_d, S_b)$ was defined as the Pearson correlation between the variables Δ_d and S_b in the simulated lineage. We adopted the same definition for the initiation adder correlation $\rho(\delta_i, s_i)$. Eventually, we found that deviations in the autocorrelation of initiation size per *ori* s_i from 0.5 significantly affected the division adderness. In contrast, deviations from adder resulting from other perturbations were weaker or less systematic, reinforcing the general robustness of adder observed in our inhibition experiments (Fig. 1D). This sensitivity of adder to s_i autocorrelation is clearly seen in the fraction of physiological space represented by adder (Fig. 2A). It is also intuitive since in the Helmstetter-Cooper model, division timing is regulated by chromosome replication initiation. As reference physiological values, we used experimental measurements obtained for strain NCM3722 in slow growth condition (MOPS minus NH_4Cl, 0.4 % glucose, 5 mM arginine). Namely, where appropriate we parametrized the joint probability distribution using the mean and coefficient-of-variations:

Variable	λ	τ_{cyc}	s_i
Mean	0.693	0.7	1
CV	15%	15%	10%

and the Pearson cross-correlations and autocorrelations:

Pearson correlation	Value
$\rho(\lambda,\tau_{cyc})$	-0.5
$\rho(\lambda,s_i)$	-0.2
$\rho(\tau_{cyc},s_i)$	-0.3
$\rho(\lambda^{(n+1)},\lambda^{(n)})$	0.5
$\rho(\tau_{cyc}^{(n+1)},\tau_{cyc}^{(n)})$	0.3
$\rho(s_i^{(n+1)},s_i^{(n)})$	0.5

Note that we chose the generation time as unit of time and the cell size per origin at initiation as unit of volume. For this particular condition, the generation time was ln(2)/ $\langle\lambda\rangle$ = 112 minutes and the cell size per origin at replication initiation was s_i = 0.30 μm^3.

Analysis of FtsZ oscillation experiment results

Let us consider a single cell, experiencing a switch in induction, corresponding to a change of steady-state concentration from c^* to c^{**}. Denoting S_{ind} the cell size reached when the switch in induction occurs, by applying Eq. 22 and Eq. 23 from the Supplemental Information III.B, we obtain:

$$S_{\mathrm{d}} - S_{\mathrm{b}} = \Delta_{\mathrm{d}}^{**} - (S_{\mathrm{ind}} - S_{\mathrm{b}})\left(\frac{\Delta_{\mathrm{d}}^{**}}{\Delta_{\mathrm{d}}^{*}} - 1\right),$$

where $\Delta_d^* = N_0/(2c^*)$ and $\Delta_d^{**} = N_0/(2c^{**})$ are the added size in each induction phase. Assuming exponential elongation of cell size at the rate λ, we may express:

$$S_{\mathrm{ind}} - S_{\mathrm{b}} = S_{\mathrm{b}}\left(e^{\lambda a_{\mathrm{ind}}} - 1\right),$$

where a_{ind} is the age of the cell when the switch in induction occurs. We therefore obtain for the conditional average:

$$\langle S_{\mathrm{d}} - S_{\mathrm{b}} | S_{\mathrm{b}}\rangle = \Delta_{\mathrm{d}}^{**} - A\left(\frac{\Delta_{\mathrm{d}}^{**}}{\Delta_{\mathrm{d}}^{*}} - 1\right) S_{\mathrm{b}},$$

where $A = \langle e^{\lambda a} - 1\rangle$, and therefore $A > 0$.

Effect of ClpX on cell size homeostasis

In the presence of ClpX, we consider that division proteins are actively degraded at a rate μ. Denoting N the copy number of division proteins, the balanced biosynthesis of division proteins is modified to:

$$\frac{\mathrm{d}N}{\mathrm{d}t} = c^* \frac{\mathrm{d}S}{\mathrm{d}t} - \mu N.$$

Assuming that the cell volume grows exponentially at the rate λ, the previous ODE can be solved, and one obtains the following functional relation between copy number and cell volume:

$$S(t) = \frac{1}{c^*}\left(1 + \frac{\mu}{\lambda}\right)\left(N(t) - N_{\mathrm{b}} e^{-\mu t}\right) + S_{\mathrm{b}} e^{-\mu t},$$

where $N_b = N(t=0)$ is the copy number at cell birth and $S_b = S(t=0)$ is the cell volume at cell birth. We assume even partitioning of division proteins at division, so that their number at birth is half the threshold:

$N_b = N_0 / 2$. We can now get some insight on cell size homeostasis by considering the two limiting cases (1) $\mu \ll \lambda$ and (2) $\mu \gg \lambda$.

In case (1), we obtain to order zero in μ/λ that $S_d - S_b = N_0/(2c^*)$, which is the adder model. On the contrary in case (2), we obtain asymptotically: $S_d = (\mu/\lambda) \cdot N_0/c^*$, which is the sizer model. In summary, the cell size behavior transitions from the adder model to the sizer model when active degradation of division proteins is introduced.